CRISPR-targeted mutagenesis of mitogen-activated protein kinase phosphatase 1 improves both immunity and yield in wheat

Saifei Liu[1,2], Fengfeng Zhang[1], Jiaxuan Su[1], Anfei Fang[1], Binnian Tian[1], Yang Yu[1], Chaowei Bi[1], Dongfang Ma[3], Shunyuan Xiao[4,5],* iD and Yuheng Yang[1],* iD

[1]Key Laboratory of Agricultural Biosafety and Green Production of Upper Yangtze River (Ministry of Education), College of Plant Protection, Southwest University, Chongqing, China

[2]Institute for Plant Sciences, Cluster of Excellence on Plant Sciences, University of Cologne, Cologne, Germany

[3]Hubei Collaborative Innovation Center for Grain Industry/College of Agriculture, Yangtze University, Jingzhou, Hubei, China

[4]Institute for Bioscience and Biotechnology Research, University of Maryland, Rockville, Maryland, USA

[5]Department of Plant Science and Landscape Architecture, University of Maryland, College Park, Maryland, USA

Summary

Plants have evolved a sophisticated immunity system for specific detection of pathogens and rapid induction of measured defences. Over- or constitutive activation of defences would negatively affect plant growth and development. Hence, the plant immune system is under tight positive and negative regulation. MAP kinase phosphatase1 (MKP1) has been identified as a negative regulator of plant immunity in model plant *Arabidopsis*. However, the molecular mechanisms by which MKP1 regulates immune signalling in wheat (*Triticum aestivum*) are poorly understood. In this study, we investigated the role of TaMKP1 in wheat defence against two devastating fungal pathogens and determined its subcellular localization. We demonstrated that knock-down of *TaMKP1* by CRISPR/Cas9 in wheat resulted in enhanced resistance to rust caused by *Puccinia striiformis* f. sp. *tritici* (*Pst*) and powdery mildew caused by *Blumeria graminis* f. sp. *tritici* (*Bgt*), indicating that *TaMKP1* negatively regulates disease resistance in wheat. Unexpectedly, while *Tamkp1* mutant plants showed increased resistance to the two tested fungal pathogens they also had higher yield compared with wild-type control plants without infection. Our results suggested that TaMKP1 interacts directly with dephosphorylated and activated TaMPK3/4/6, and TaMPK4 interacts directly with TaPAL. Taken together, we demonstrated TaMKP1 exert negative modulating roles in the activation of TaMPK3/4/6, which are required for MAPK-mediated defence signalling. This facilitates our understanding of the important roles of MAP kinase phosphatases and MAPK cascades in plant immunity and production, and provides germplasm resources for breeding for high resistance and high yield.

Introduction

Plants have evolved complex mechanisms to recognize invading pathogens and mount appropriate defence responses to fight off infection (Dodds and Rathjen, 2010; Schwessinger and Ronald, 2012). They detect the presence of pathogen/microbe-associated molecular patterns (PAMPs/MAMPs) and pathogen effector proteins, and subsequently initiate a diverse array of defence responses, via highly conserved signalling mechanisms (Teixeira et al., 2019; Zhou and Zhang, 2020). The recognition of PAMPs by plasma membrane-localized pattern recognition receptors (PRRs) ensues PAMP-triggered immunity (PTI). Adapted pathogens employ secreted effectors to subvert PTI. In response, plant intracellular immune receptors detect specific pathogen effectors, resulting in effector-triggered immunity (ETI) (Li et al., 2020; Monaghan and Zipfel, 2012). There are several early signalling events and defence responses during PTI and ETI. These include intracellular calcium flux, activation of the mitogen-activated protein kinase (MAPK) cascades, production

of extracellular reactive oxygen species (ROS), and increased biosynthesis of salicylic acid (SA). ETI is often collimated with hypersensitive response (HR), which is rapid and localized cell death at the site of infection that plays an important role in containing invading pathogens, especially biotrophic fungi (Wang et al., 2020).

MAPK activation is one of the earliest signalling events that function downstream of immune receptors and transduce phytopathogenic stimuli into cellular defence responses (Zhang et al., 2018). MAPK cascades are three-kinase modules consisting of MAPK kinase kinases (MKKKs/MEKKs), MAPK kinases (MKKs/MEKs), and MAPKs (Ichimura et al., 2002). In MAPK cascades, MAPKs are phosphorylated and activated by MAPKKs, which are in turn activated by their upstream kinases MAPKKKs (Zhang and Klessig, 2001). Numerous members of MAPK cascades have been reported to be involved in defence signalling. Notably, most research in the past has been focused on two hallmark parallel MAPK cascades (Devendrakumar et al., 2018). In *Arabidopsis*, the MKKK3/5-MKK4/5-MPK3/6 cascade

downstream of multiple plant receptor kinases positively regulates both PTI and ETI responses (Sun *et al.*, 2018; Zhang and Klessig, 2001). The *Arabidopsis* MEKK1-MKK1/2-MPK4 cascade is another best studied MAPK cascade involved in flg22-induced immune signalling and mechanical wounding responses linked to ROS signalling (Takahashi *et al.*, 2011).

MAPKs are activated through sequential phosphorylation and deactivated upon dephosphorylation by phosphatases. Three types of protein phosphatases are known to deactivate MAPK. These include tyrosine phosphatases, serine/threonine phosphatases, and dual specificity phosphatases (DSPs) that are capable of removing the phosphate groups from phosphoserine, phosphothreonine, and phosphotyrosine residues (Keyse, 2000). MAPK phosphatase 1 (MKP1), belonging to the group of DSPs, has been previously described as a broad negative regulator of plant stress responses through its regulation of MAPK signalling. In *Arabidopsis*, AtMKP1 (At3g55270) has been shown to be a crucial regulator of AtMPK6 (At2g43790) activity, determining the outcome of the cellular reaction and the level of genotoxic resistance (Ulm *et al.*, 2001, 2002). In rice, OsMKP1 negatively regulates MAPK-mediated phosphorylation of the transcription factor MYB4 which in turn negatively regulates vascular lignification through inhibiting lignin biosynthesis and vascular resistance to *Xanthomonas oryzae* pv. *Oryzicola* (*Xoo*) (Lin *et al.*, 2022). OsMKP1 also negatively regulates SA- and ROS-dependent mesophyll resistance to *Xoo* via dephosphorylation of MAPK (Lin *et al.*, 2022; Zhang *et al.*, 2022), which is consistent with earlier studies that AtMKP1 interacts with its targets MPK3 (At3g45640) and MPK6, thereby negatively regulating SA biosynthesis and ROS to maintain the best balance between growth and pathogen resistance (Anderson *et al.*, 2011; Bartels *et al.*, 2009). Phosphorylation of AtMKP1 was also shown to be required for PAMP responses and bacteria resistance (Escudero *et al.*, 2019; Jiang *et al.*, 2017), and increased bacterial resistance in *Atmkp1* was found to be attributable to a decrease in the extracellular accumulation of bioactive metabolites that induce the bacteria's type III secretion system critical for bacterial pathogenicity (Anderson *et al.*, 2014). Notably, AtMKP1 was also reported to be phosphorylated and activated by its physiological substrate, MPK6 (Park *et al.*, 2011). In addition, AtMKP1 directly regulates RBOHD, an NADPH oxidase for ROS production during PTI process (Escudero *et al.*, 2019). A more recent study showed that AtMKP1 promotes osmotolerance by suppressing the PAD4-independent immune response activated by MPK3/6 (Uchida *et al.*, 2022).

Heterologous expression of *TdMKP1* isolated from durum wheat (*Triticum durum*) in *Arabidopsis* was shown to increase salt stress tolerance of the transgenic plants (Zaidi *et al.*, 2016). TdMKP1 contains a canonical 14–3-3 binding motif and was shown to interact with and regulated by 14–3-3 proteins, a family of highly conserved acidic proteins that act as dynamic coordinators of many biological processes (Ghorbel *et al.*, 2017). In gel assays showed that TdMKP1 could be regulated by calmodulin, bivalent cations and possibly TdMPK3 but its phosphorylation status seemed dispensable for an optimal phosphatase activity (Ghorbel *et al.*, 2019). To date, whether *MKP1* in wheat especially the allohexaploid bread wheat (*Triticum aestivum*) also plays an important role in negative regulation of immune signalling similar as *AtMKP1* in *Arabidopsis* has yet to be determined.

In this study, we identified three *TaMKP1* homoeologous genes in the genome of bread wheat and examined their expression patterns in response to pathogen infection. More importantly, we obtained definitive evidence to indicate that *TaMKP1* plays a role in negative regulation of defence responses via inhibiting the activation of three key components of MPK3, MPK4 and MPK6 that function in two parallel MAPK cascades. We also generated wheat *mkp1* plants by clustered regularly interspaced short palindromic repeats/CRISPR-associated 9 (CRISPR/Cas9) technology and found that while *Tamkp1* plants showed increased resistance to biotrophic rust and powdery mildew fungi, surprisingly, they also displayed improved wheat agronomic traits (plant height, ears and grain weight). The research findings presented in this study suggest novel molecular mechanisms that underlie the interplay between growth and defence in wheat and hint new strategies for improving both disease resistance and yield characteristics through genetic manipulation of *TaMKP1*.

Results

TaMKP1 expression is rapidly induced upon fungal infection

The genome of allohexaploid bread wheat contains three *MKP1* homoeologs (*TraesCS1A02G045300*, *TraesCS1B02G058600* and *TraesCS1D02G046000*) with ~97% nucleotide sequence identity between each other (Figure S1). The three deduced TaMPK1 proteins show ~54% sequence identity to AtMKP1, and were designated TaMKP1a, TaMKP1b and TaMKP1d, respectively, according to their chromosomal (Figure 1a). Phylogenetic analysis with the three TaMKP1 homoeologs and 16 representative MPK1s from other plant species showed that TaMKP1d is most closely related to predicted MKP1 proteins from *Aegilops tauschii* (which contributes to the wheat D genome) while TaMKP1a is most closely related to MPK1 form from Durum wheat *Triticum turgidum* (Figure 1b).

To assess the role of *TaMKP1* in the regulation of disease resistance, wheat plants were challenged with a virulent *Puccinia striiformis* f. sp. *tritici* (*Pst*) race (CYR34). The expression level of *TaMKP1a* in the inoculated leaves rapidly increased by more than 4 times at 12 h-post inoculation (hpi), and then gradually dropped back to the level prior to infection. *TaMKP1b* and *TaMKP1d* expression was upregulated at 24 hpi and reached a maximum at 48 hpi, with 8.7- and 6.7-fold increases, respectively (Figure 1c). This result implies that *TaMKP1* may be involved in early responses of wheat to fungal infection. The total transcripts of *TaMKP1* were found to be most abundant in mature leaves, which is over 2-fold higher ($P < 0.05$) than those of root tissue. In grains and culms, the total transcripts of *TaMKP1* were slightly less abundant compared to those in roots (Figure S2).

Knocking down TaMKP1 results in enhanced resistance in wheat

To determine the role of *TaMKP1* in regulating defence responses in wheat, a well-established virus-induced gene silencing (VIGS) system was employed. Specifically, two artificial microRNA (amiRNA) genes that aim to target all of the three *TaMKP1* homoeologs were made and expressed in wheat using the BSMV-mediated gene-silencing system. At 12 dpi with BSMV, leaf photo-bleaching was observed in plants inoculated with the virus harbouring the amiRNA construct targeting the wheat phytoene desaturase gene (*TaPDS*), and mild chlorotic mosaic phenotypes were apparent on leaves inoculated with the virus carrying no insert or one of the two amiRNA constructs targeting *TaMKP1* (Figure 2a), indicating that the BSMV-based VIGS system was
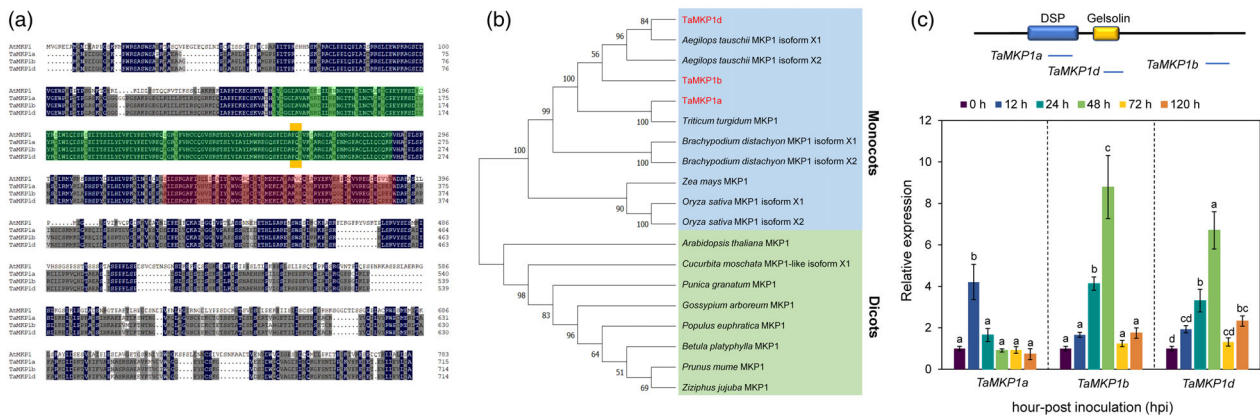
Figure 1 Identification of bread wheat MKP1 (TaMKP1) homologues and expression patterns. (a) Multiple alignment of the amino acid sequences of TaMKP1a, TaMKP1b, TaMKP1d, and AtMKP1. The green box indicates the DSP (dual-specificity phosphatase) domain, the red box represents the Gelsolin repeat region, and the yellow region represents the FXF motif. (b) Phylogenetic analysis between TaMKP1 and other plants. (c) The expression level of *TaMKP1* induced by *Pst* CYR34. TaMKP1 contains DSP and Gelsolin domains, and the horizontal line under the domain indicates the *TaMKP1* RT-qPCR amplified fragment.
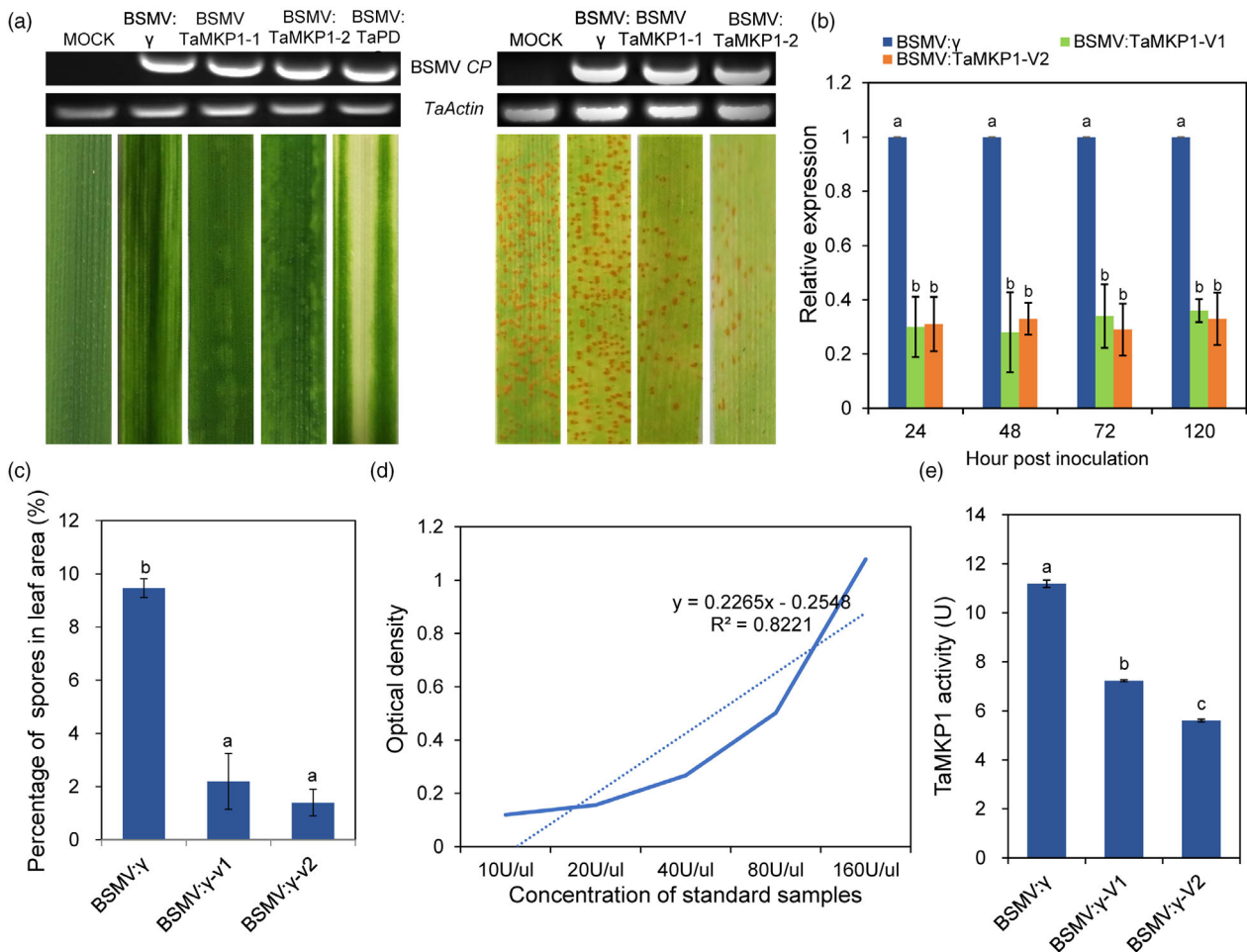

Figure 2 The silencing of *TaMKP1* enhances the resistance of wheat to pathogens. (a) Wheat leaf symptoms after virus inoculation and phenotype of wheat leaves silenced for *TaMKP1* gene infected by *Pst*. (b) Relative transcript levels of *TaMKP1* in control and TaMKP1-silenced plants. (c) The percentage of *Pst* urediniospores on wheat leaves. (d) The standard curve for MKP1 enzyme activity. (e) Changes in MKP1 enzyme activity in silenced plants.

working. Subsequently, the fourth leaves were inoculated with fresh urediniospores of *Pst*-CYR34. As expected, numerous uredia were produced on mock (BSMV-Y) leaves at 14 dpi. By contrast,

noticeably less *Pst* uredia were observed on leaves infected with BSMV:TaMKP1-V1 or BSMV:TaMKP1-V2 (Figure 2a). QRT-PCR showed that the transcription levels of *TaMKP1* in the fourth

leaves of plants inoculated with either *BSMV:TaMKP1-V1* or *BSMV:TaMKP1-V2* were suppressed below 35% of that of the mock plants at 24, 48, 72, and 120 hpi with *Pst*-CYR34 (Figure 2b). When TaMKP1 was silenced, the proportion of surface spores in leaves of BSMV-TaMKP1 plants decreased significantly compared with control plants (Figure 2c). In addition, the proportion of spore heaps and the activity of the TaMKP1 enzyme in *TaMKP1*-silenced plants showed a significant decrease compared to those in the mock plants (Figure 2d,e).

Knocking out TaMKP1 by CRISPR/Cas9 results in clear enhanced resistance

To more definitively assess the role of *TaMKP1* in regulation of defence signalling in wheat, CRISPR/Cas9 gene-editing was used to knock out *TaMKP1* in wheat. To achieve this, a single guide RNA was designed to target an exonic region where the nucleotide sequence is identical among the three *TaMKP1* genes (Figure 3a). Successful transformation of Fielder immature
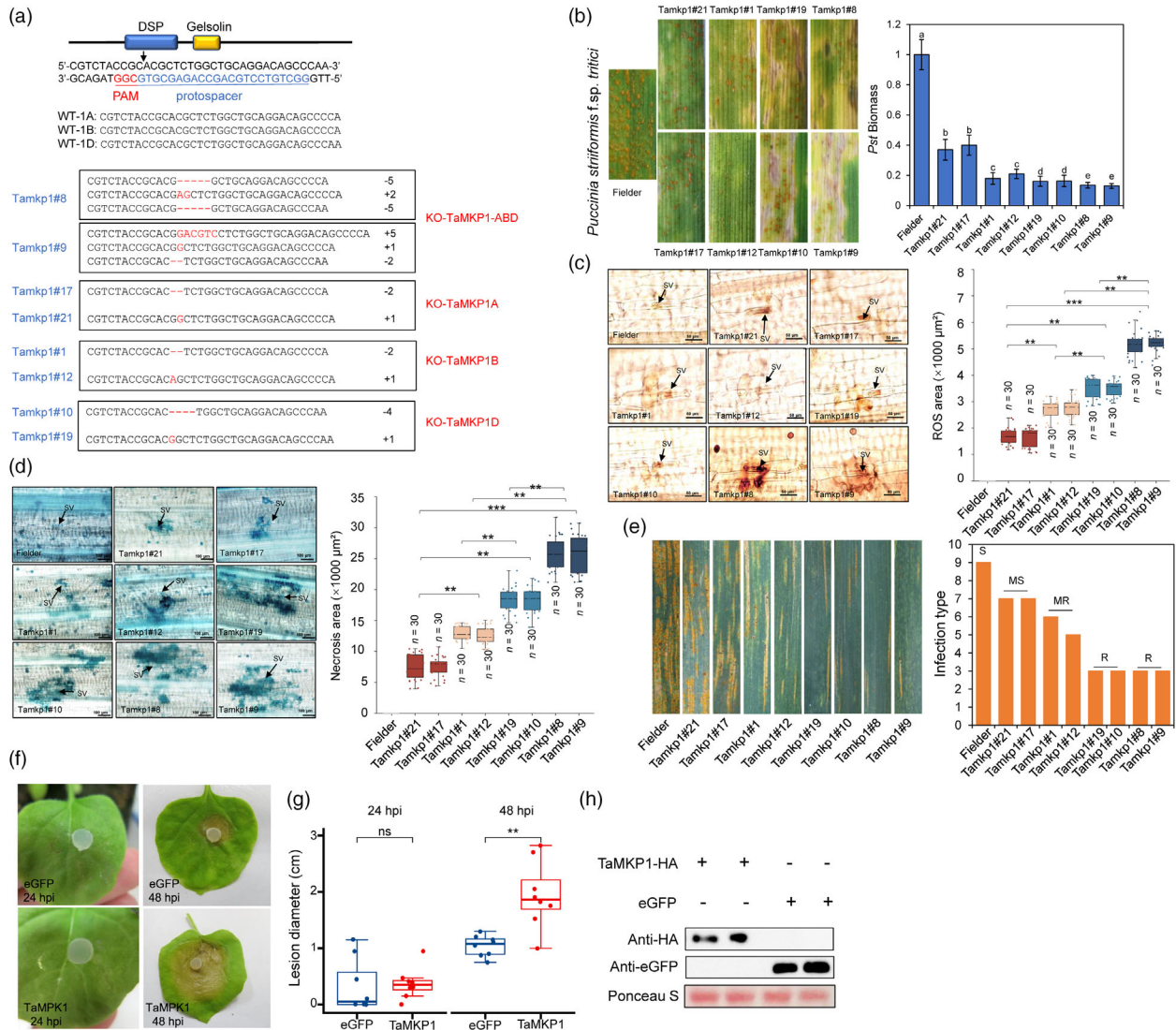

Figure 3 TaMKP1 plays a negative regulatory role in the interaction between plants and pathogens. (a) Selection of TaMKP1 mutation targets and identification of mutation types in *TaMKP1* homologues. Deleted nucleotides are represented by "-". Inserted nucleotides are highlighted in red. The numbers on the right indicate the number of nucleotides involved in the indel events, represented by "+" or "−". (b) Leaf phenotypes of *aaBBDD*, *AAbbDD*, *AABBdd* and *aabbddd* compared with Fielder at 14 dpi with *Pst* CYR34, and *Pst* biomass statistics. (c) ROS production was observed in *Pst*-infested leaves at 24 hpi. (d) Histological observation of host cell death on the *Tamkp1* leaves at 120 hpi with CYR34. Student's *t*-tests were used to assess the differences between knockdown plants and control plants. Significance levels were denoted as * for $P < 0.05$, ** for $P < 0.01$, *** for $P < 0.001$ and ****for $P < 0.001$. SV refers to substomatal vesicle. (e) Characterization of *Tamkp1* plants for disease resistance at the adult plant stage. S represents susceptible, MS represents moderately susceptible, MR represents moderately resistant, and R represents resistant. (f) Observations on the infection phenotype in overexpressed *TaMKP1 Nicotiana benthamiana* inoculated with *Sclerotinia sclerotiorum*. (g) Statistical analysis of lesion diameter following inoculation with *S. sclerotiorum*. ** indicate a significant difference ($P < 0.01$) according to Student's *t*-test. (h) Western blot was performed to confirm the expression of *TaMKP1* in *N. benthamiana*.

embryos was achieved through *Agrobacterium* mediated transformation, resulting in T0 events. Mutant lines were identified using the bar gene test strip (Figure S3). To identify indel mutations in the target genes, specific primers were designed to amplify and sequence the target region of the three *TaMPK1* homeologs. Among eight transgenic T1 lines analysed by targeted sequencing, a frameshift indel resulting in an earlier stop codon in each of the three *TaMPK1* homeologs were found in two lines (#8 and #9), while one frameshift indel in one of the three *TaMKP1* homeologs was identified in the remaining six lines (Figures 3a and S4). T2 progenies of the 8 T1 lines with the respective homozygous mutations were obtained and subjected to infection tests with *Pst* CYR34. For simplicity, *aa*, *bb* and *dd* are used to denote homozygous knockout mutations in *TaMKP1* in the A, B and D genome, respectively. Not surprisingly, while *aabbdd* plants of line #8 and #9 showed the highest levels of resistance, which was reflected in lower fungal biomass at 14 dpi, which decreased by 86.5% and 86%, respectively. *AABBdd* plants from line #10 and #19 exhibited the second lowest incidence and fungal biomass, which decreased by 83.9% and 83.7%, respectively (Figure 3b). *AAbbDD* plants from line #1 and #12 and *aaBBDD* plants from line #17 and #21 were also significantly less susceptible compared to the WT Fielder plants, even though they were not as resistant as *aabbdd* and *AABBdd* plants (Figure 3b). DAB and Trypan Blue staining were used to respectively assess the *in-situ* accumulation of hydrogen peroxide (H_2O_2) and HR cell death in infected leaves at 24 hpi. While no obvious H_2O_2 was detected in WT plants, plants of the *aabbdd* genotype developed massive H_2O_2 with the highest positive area, followed by plants of the *AABBdd*, *AAbbDD* and *aaBBDD* genotypes (Figure 3c). Results of HR cell death was consistent with the development of macro-lesions in *Pst*-infected leaves (Figure 3b) and were also highly similar to patterns of H_2O_2 production and accumulation (Figure 3d).

To confirm the enhanced resistance to virulent *Pst* race CYR34 in the *TaMKP1* knockout lines is indeed due to PTI de-repression, WT and mutant plants of the above-described genotypes were treated with chitin or flg22. Our results showed that both chitin and flg22 more strongly induced H_2O_2 production in the mutant plants of different genotypes than WT plants (Figure S5). This result is consistent with more pronounced expression of *TaCERK1* and *TaRLCK185* (which is indicative of hyperactive chitin-induced immune signalling) upon chitin treatment and *TaFLS2* and *TaMEKK1* (which is indicative of hyperactive flg22-induced immune signalling) upon flg22 treatment in the mutant plants compared with WT plant (Figure S5).

T2 plants of the *TaMKP1* knockout lines were subjected to mixed infection tests at the adult stage with four prevalent and severe *Pst* strains (CYR31, CYR32, CYR33 and CYR34). T2 plants of the *aabbdd* genotype and *AABBdd* genotypes supported least *Pst* urediniospores, while T2 plants of the *AAbbDD* and *AABBDD* genotypes also showed significantly reduced susceptibility to prevalent *Pst* races when compared the WT plants (Figure 3e). These results further demonstrated that *TaMKP1* homeologs are negative regulators of resistance against *Pst* in wheat and suggested that *TaMKP1d* play the largest role among the three homeologs. To see if the enzymatic function of MKP1 is indeed conserved across plant species, we ectopically expressed *TaMKP1* (which is identical to TaMKP1b and TaMKP1d at the protein level) in *Nicotiana benthamiana* leaves via *Agrobacterium*-mediated transient expression. The *TaMKP1* gene was translationally in-frame fused with a C-terminal hemagglutinin (HA) tag and

TaMKP1-HA fusion gene construct was transiently expressed in *N. benthamiana* leaves along with the *eGFP* construct (as control). Twenty-four hours after *Agroinfiltration*, a *Sclerotinia sclerotiorum* strain virulent on *N. benthamiana* was inoculated on the infiltrated leaves. Larger lesions were observed on the leaves expressing *TaMKP1* compared with those expressing *eGFP* (Figure 3f,g). Western blot analysis showed that both TaMKP1-HA and eGFP were expressed in the infiltrated leaves (Figure 3h). This result suggested that TaMKP1 from wheat is capable of dephosphorylating relevant *N. benthamiana* proteins and consequently downregulating immune responses in distantly dicot plant species.

Next, plants of the *Tamkp1* mutants inoculated with a virulent powdery mildew *Blumeria graminis* f. sp. *tritici* (*Bgt*) to evaluate the scope and effectiveness of their enhanced resistance. The results indicated that *Tamkp1* plants have significantly reduced susceptibility to compared to the WT as shown by visual scoring of the infected leaves and *Bgt* biomass (Figure 4a). Similar to the infection phenotypes with *Pst*-CYR34, the number and size of micro-colonies of *Bgt* mycelium on leaves of the *aabbdd* mutant plants were most significantly reduced, followed by those of *AABBdd*, and then *AAbbDD* and *aaBBDD* genotypes compared to the WT (Figure 4b,c), while *Bgt*-induced HR cell death in the infected leaves exhibited a reverse tendency based on visualization of cell death stained by trypan blue (Figure 4d). These results further substantiated our conclusion that knocking out *TaMKP1* genes in wheat results in enhanced resistance to biotrophic fungal pathogens.

Nucleus-localized TaMKP1 represses immune signalling

The N-terminal domain of human MKP-1 is responsible for both nuclear localization and for binding of its MAPK substrates (Kim and Asmis, 2017). Durum wheat MKP1 was localized in the nucleus and interacts with MPK3/6 (Zaidi *et al*., 2016). To investigate whether nuclear localization of TaMKP1 is required for repressing defence signalling, a nuclear localization signal (NLS) or a nuclear export signal (NES) was added to C-terminus of TaMKP1-GFP to make TaMKP1-GFP-NLS (or NES) constructs. Each of the two constructs were co-expressed with the nuclear marker H2B-mCherry (Long *et al*., 2019) in *N. benthamiana* leaves. Fluorescence microscopy showed that as expected, TaMKP1-GFP-NLS was localized in the nucleus, whereas TaMKP1-GFP-NES was found in the cytoplasm with little GFP signal seen in the nucleus (Figure 5a). Then, the infiltrated leaves were inoculated with *S. sclerotiorum*. Interestingly, leaves transiently expressing TaMKP1-GFP-NLS displayed significantly larger infection lesions compared with those expressing the TaMKP1-GFP-NES (Figure 5b). Gel blot analysis showed that TaMKP1-GFP-NES was expressed and distributed in both the cytoplasm and nucleus, mainly in the cytoplasm, while TaMKP1-GFP-NLS was only in the nucleus (Figure 5c). These observations suggest that TaMKP1 proteins mainly act to repress defence signalling in the nucleus.

TaMKP1 interacts with, dephosphorylates and activates TaMPK3, TaMPK4 and TaMPK6

Previous studies showed that AtMKP1 interacts with its dominant substrate, AtMPK6, to repress defence/stress signalling in *Arabidopsis* (Anderson *et al*., 2011; Ulm *et al*., 2002). To identify wheat MAPKs targeted by and interacting with TaMKP1, wheat genes encoding core members of the MAPK cascades (i.e. TaMPK3, TaMPK4 and TaMPK6) were identified *in silico* (Figure S6) and cloned into the prey vector pGBKT7 for directed
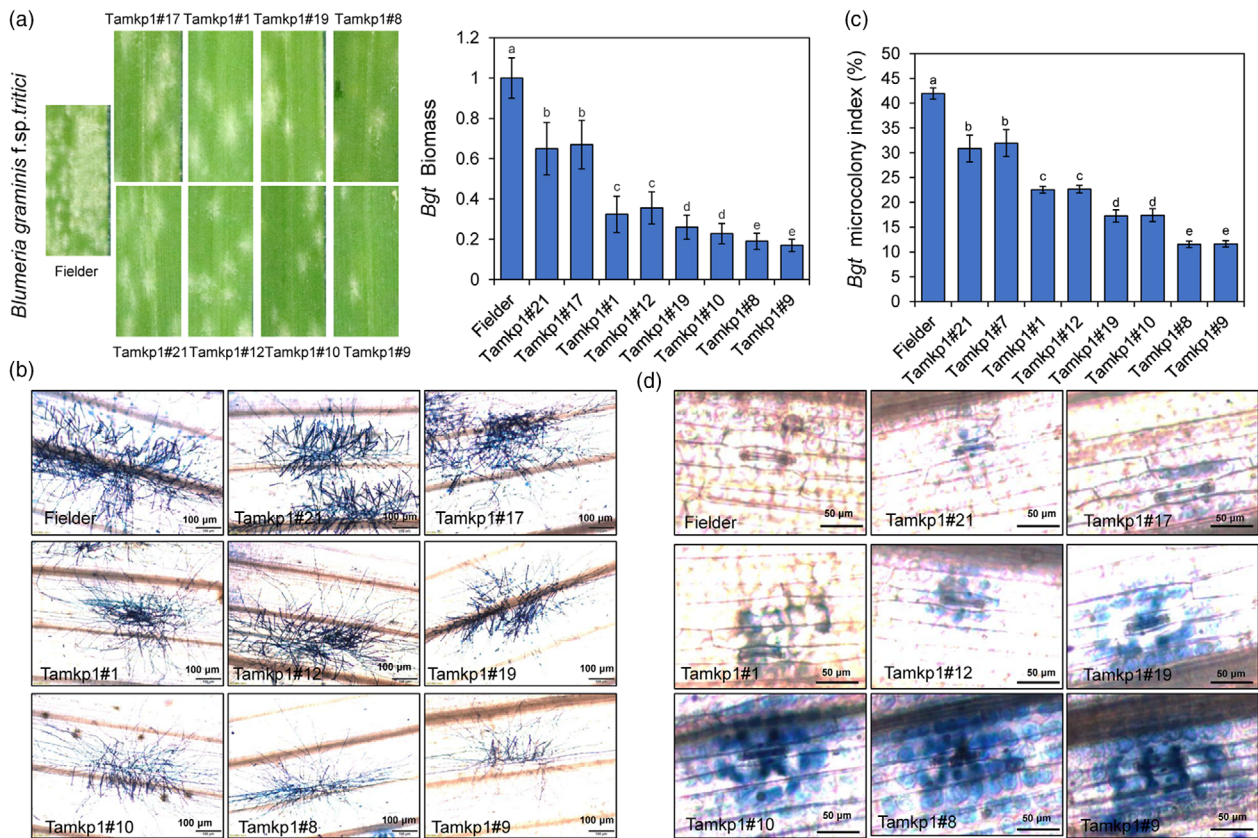
Figure 4 *Tamkp1* plants demonstrate broad-spectrum disease resistance. (a) Leaf phenotypes of *Tamkp1* plants compared with Fielder at 7 dpi with *Bgt*, and *Bgt* biomass statistics. (b) The leaves of T2 generation of *Tamkp1* plants were infected, and 7 dpi, they were stained with trypan blue to make fungal structures visible. (c) Statistical analysis of *Bgt* microcolony formation on Fielder and *Tamkp1* leaves. (d) Host cell death on the *Tamkp1* leaves with *Bgt*.
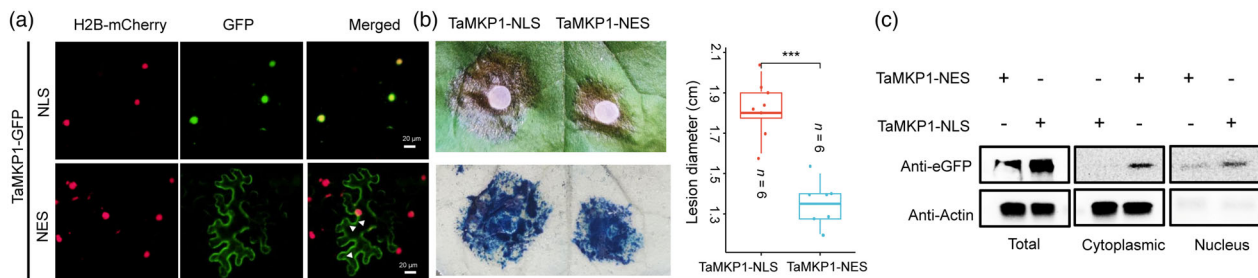

Figure 5 Nucleus-localized TaMKP1 contributes to plant susceptibility against pathogens. (a) Observation of TaMKP1 nuclear localisation and nuclear export signals. Scale bar: 20 μm. (b) TaMKP1-nuclear localisation and nuclear export signal region of the lesion phenotype and statistical analysis of lesion diameter **** indicate a significant difference ($P < 0.0001$) according to Student's *t*-test. (c) Western blot analysis to verify the expression of TaMKP1-NES and TaMKP1-NLS in plants.

yeast two-hybrid (Y2H) assays with *TaMKP1a* cloned into the bait vector pGADT7. Interestingly, as shown in Figure 6a, TaMKP1 was able to interact with TaMPK3, TaMPK4 and TaMPK6 in yeast cells (Figure 6a).

To confirm whether TaMKP1 interacts with TaMPK3, TaMPK4, and TaMPK6 *in planta*, bimolecular fluorescence complementation (BiFC) assay was performed. To this end, *TaMKP1a* was translationally fused with the C-terminal fragment of YFP, and *TaMPK3*, *TaMPK4* and *TaMPK6* were translationally fused with the N-terminal fragment of YFP. The *cYFP-TaMKP1a* fusion gene was co-expressed with *nYFP-TaMPK3* or *nYFP-TaMPK4*, or *nYFP-TaMPK6* in *N. benthamiana* leaves. At 48 h after agroinfiltration, strong YFP signal was predominantly detected in the nuclei of leaf

epidermal cells co-expressing any of the three above combinations (Figure 6b), indicating that TaMKP1 interacts with each of the three TaMPKs and the interaction mainly occurs in the nucleus. Similar results supporting the *in planta* direct interaction between TaMKP1 and each of the three TaMPKs were obtained using Luciferase complementation (LUC) assays (Figure 6c). To further validate the interaction of TaMKP1 and TaMPK3/4/6 *in vivo*, co-immunoprecipitation (Co-IP) assays were performed using TaMKP1 tagged with hemagglutinin (HA) and TaMPK3/4/6 tagged with FLAG via co-transient expression in leaves of *N. benthamiana*. As expected, Co-IP results showed that TaMKP1 was able to pull down the three TaMPKs, further demonstrating that TaMKP1 interacts with TaMPK3/4/6 (Figure 6d).
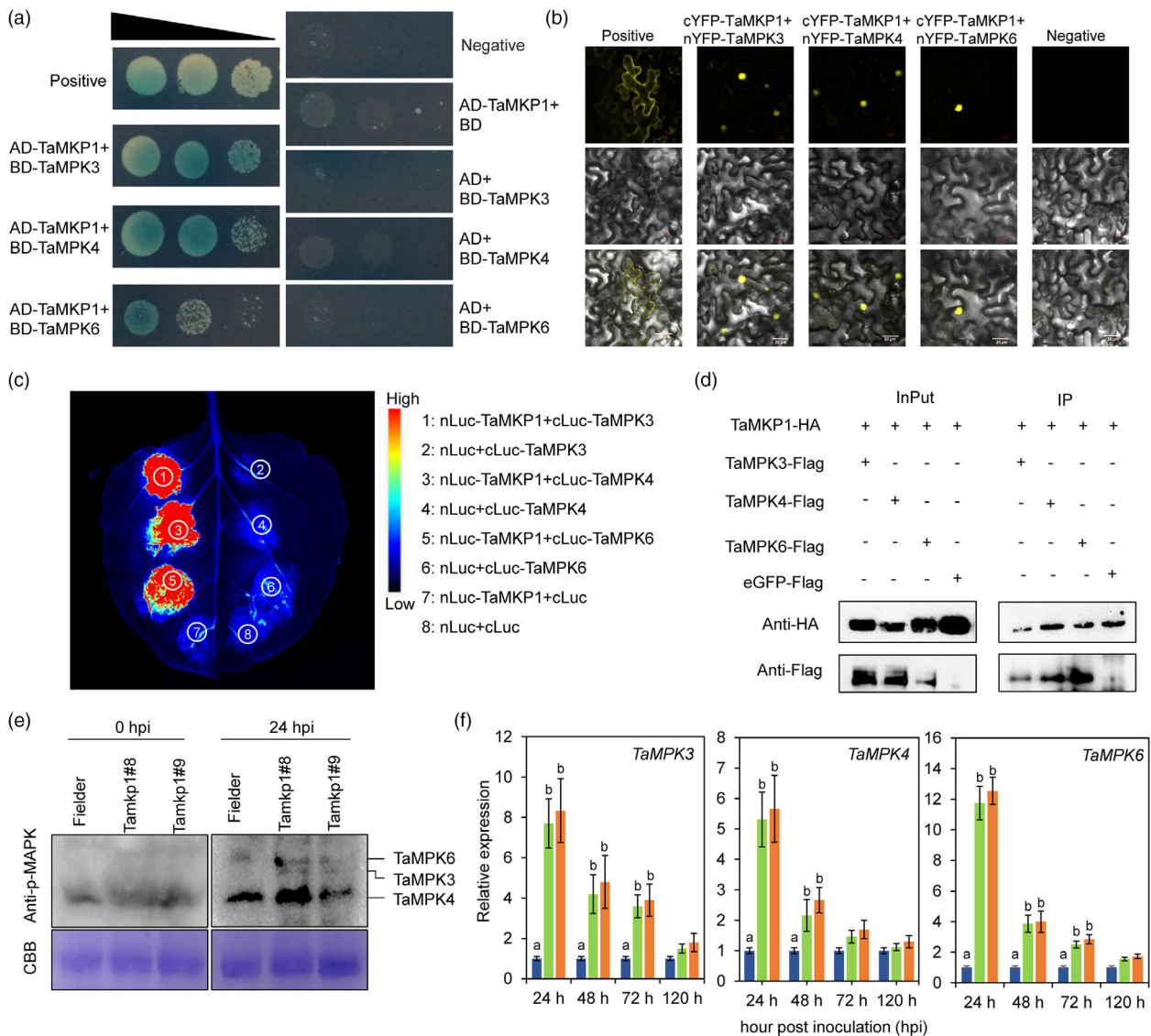
Figure 6 TaMKP1 interacts with, dephosphorylates, and activates TaMPK3/4/6. (a) Yeast Two-Hybrid (Y2H) assay was used to validate the interaction between TaMKP1 and TaMPK3/4/6 in yeast cells. (b) *In vivo* BiFC analysis of TaMKP1 interaction with TaMPK3/4/6. (c) The LUC assay confirmed the interaction between TaMKP1 and TaMPK3/4/6. (d) *In vivo* co-immunoprecipitation of TaMKP1 with TaMPK3, TaMPK4 or MPK6. (e) TaMKP1 affects phosphorylation levels of TaMPK3/4/6 *in vivo*. Immunoblot assay for MAPK phosphorylation using anti-phospho-MAPK antibodies. The *Tamkp1* plants and Filder were treated with *Pst* CYR34. Proteins were extracted from *Tamkp1* mutant and Fielder leaves at 0, and 24 h. CBB staining is shown as a protein loading control. (f) The relative transcript levels of *TaMPK3*, *TaMPK4*, and *TaMPK6* in *Tamkp1* plants.

The physical interaction of TaMKP1 with TaMPK3/4/6 suggests that TaMPK3/4/6 are authentic substrates of TaMKP1. To test whether TaMKP1 dephosphorylates TaMPK3/4/6, we analysed the phosphorylation levels of TaMPKs in *Tamkp1* plants. The results showed that *Pst* actively induced MPK3, MPK4, and MPK6 phosphorylation at higher levels in *Tamkp1* plants than that in Fielder (Figure 6e). The transcripts of *TaMPK3/4/6* genes in *Tamkp1* plants were detected using qRT-PCR. Compared to the control plants, the expression levels of *TaMPK3/4/6* significantly increased at 24 hpi and 48 hpi with *Pst* (Figure 6f).

TaMPK4 interacts with TaPAL

In recent years, a few downstream target proteins of MPK3/6 have been identified. These include transcription factors ERF3

and WRKY33 (Wang *et al.*, 2018b, 2023; Zhang *et al.*, 2021). In this study, we utilized Y2H technology to screen for interacting targets of TaMPK4 in the wheat nucleus system. As a result of this screening, we identified TaPAL. Y2H, BiFC and LUC assays were used to determine whether TaMPK3/4/6 interacts with TaPAL. Y2H assays finding that TaPAL interact with TaMPK4 but not TaMPK3/6 (Figure 7a). LUC assays supported the finding that TaMPK4 interact with TaPAL (Figure 7b). The BiFC results showed that YFP signal was distributed in the nucleus of *N. benthamiana* co-expressing nYFP-TaMPK4 with cYFP-TaPAL (Figure 7c).

Moreover, to determine whether TaMPK4 regulates TaPAL transcription, we used qRT-PCR to analyse *TaPAL* transcript levels in *Tamkp1* plants and Fielder. Compared to the corresponding controls, the *TaPAL* transcript level was up-regulated in the *Tamkp1*
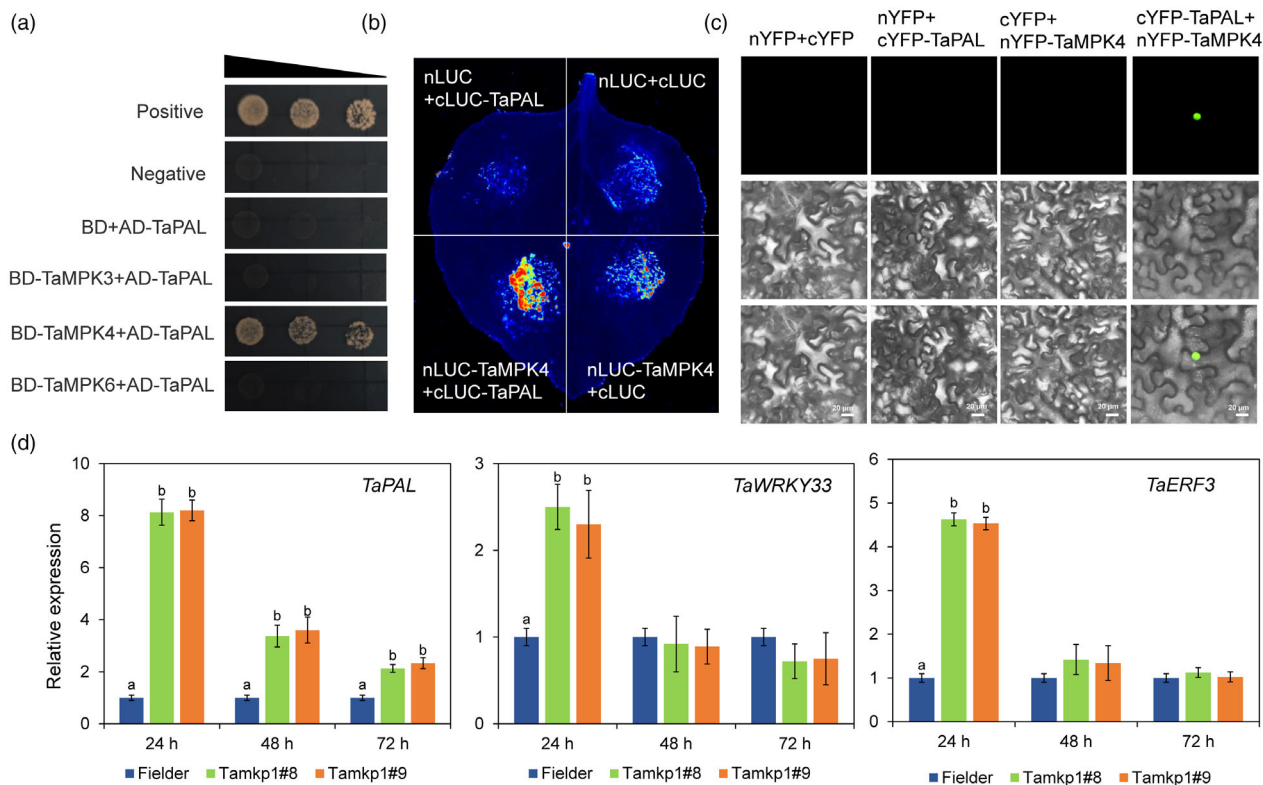
Figure 7 TaMPK4 interacts with TaPAL. (a) Y2H assay was used to validate the interaction between TaPAL and TaMPK4. (b) The LUC assay confirmed the interaction between TaPAL and TaMPK4. (c) BiFC analysis of TaPAL interaction with TaMPK4. Scale bar: 20 μm. (d) The relative transcript levels of *TaPAL*, *TaWRKY33*, and *TaERF3* in *Tamkp1* plants.

plants, suggesting that *TaMPK4* overexpression might activate *TaPAL* expression. In addition, transcript levels of *TaWRKY33* and *TaERF3* were up-regulated in *Tamkp1* plants (Figure 7d).

Wheat TaMkp1 mutants exhibit better performance in growth and reproduction

Defence activation is costly, hence there must be a defence-growth trade-off in plants (Huot *et al.*, 2014). To test if loss of *TaMKP1* genes indeed incurs a fitness cost in wheat, a field evaluation of different *TaMKP1* mutant lines was conducted along with the WT plants. During the early growth stage, all mutant lines were phenotypically similar to the WT. However, to our surprise, during the later growth stage, all mutant lines showed a slight yet significant increase in plant height. Among them, plants of the *aabbdd* lines exhibited the greatest height, followed by the *AABBdd* lines, and then the *aaBBDD* and *AAbbDD* lines (Figure 8a,d).

Consistent with the performance in plant height, all *TaMKP1* mutant lines exhibited a significant increase in spike length (Figure 8c), and in grain length, grain width, and grain yield (Figure 8b,e) compared to the WT. Interestingly, the degree of increase in those traits remained more or less the same order among the mutant lines, that is *aabbdd* (most increase), *AABBdd*, *aaBBDD*, and then *AAbbDD* (least increase). The unexpected yet exciting results from our field experiments strongly suggest that the defence-growth trade-off is not a constant and that these two contrasting traits may reconcile under certain context such as when *TaMKP1* genes in wheat are ablated.

TaMKP1 gene regulatory network and global germplasm relationships

To understand the gene regulation of *TaMKP1*, a gene regulatory network (GRN) was constructed based on wGRN (http://wheat.cau.edu.cn/wGRN/) (Chen *et al.*, 2023). GRN analysis revealed that *TaMKP1* was regulated by multiple transcription factors, with the top 6 ranked factors being calmodulin-binding transcription activator 2-like, auxin response factor 4-like, transcription factor MYC2-like, MYB family transcription factor PHL7, NAC domain-containing protein 78, and ethylene-responsive transcription factor RAP2-13 (Figure S7; Table S1). These results indicated that *TaMKP1* not only participates in the response of plants to biotic stress, but also plays an important role in other physiological processes of plants.

Wheat is a globally important staple crop. To enhance our knowledge of the genetic diversity of wheat varieties and the significance of the *TaMKP1* gene, a genomic-based germplasm network (GGNet) was constructed based on Wheat-Comp Database (http://wheat.cau.edu.cn/WheatCompDB/) (Yang *et al.*, 2022b). Fielder is one of the American cultivars (AMC). This variety has a close genetic relationship with African landrace (ASL), Asian cultivar (ASC), European cultivar (EUC), Chinese cultivar (CNC), Chinese landrace (CNL) and other germplasm resources (Figure S7). The research findings suggested that potential application prospects exist for enhancing disease resistance and increasing yield in global wheat through the modification of the *TaMKP1* gene.
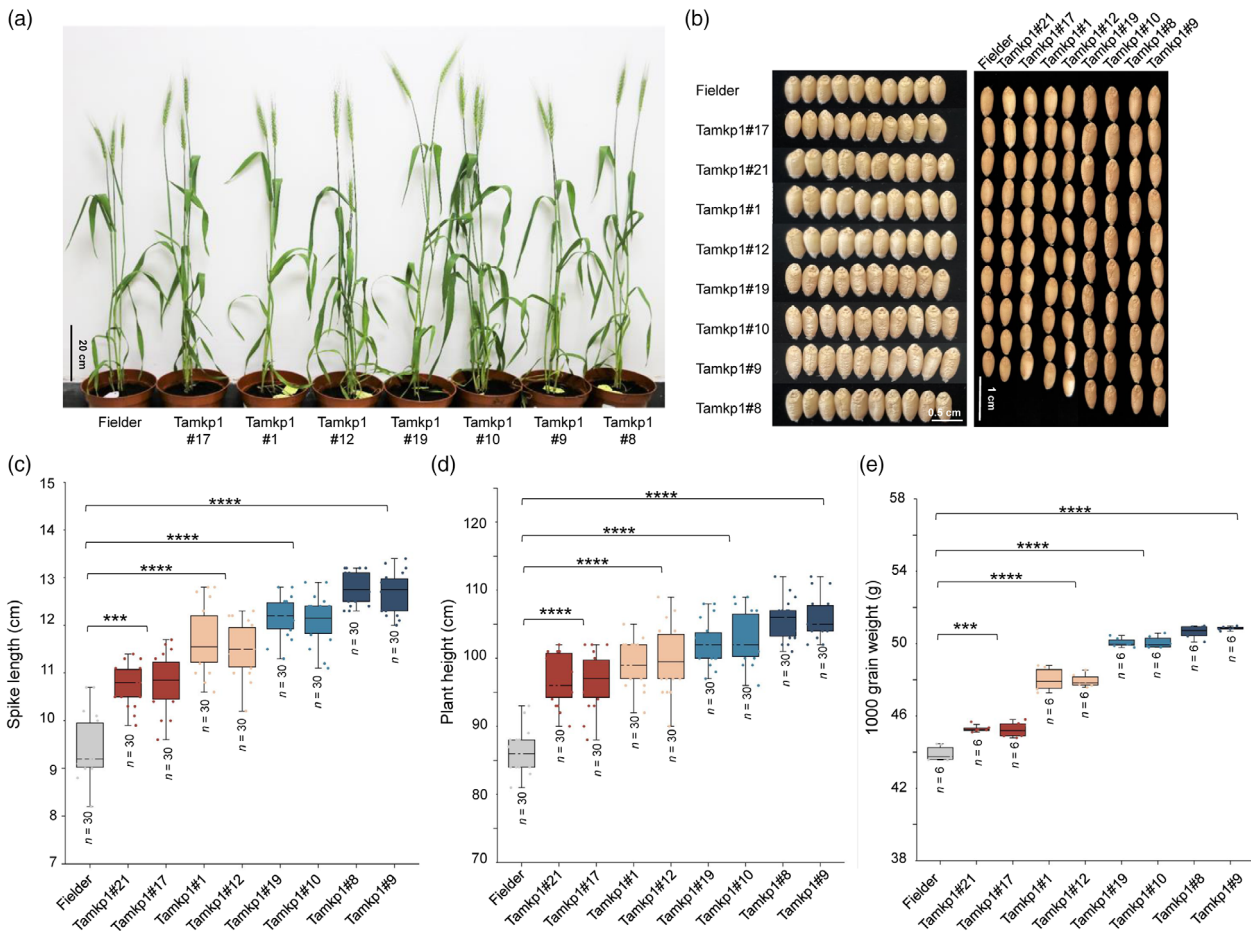
Figure 8 Field performances of the different *Tamkp1* plants. (a) The growth conditions of *Tamkp1* plants and Fielder in the field. (b) Mature paddy wheat grains of Fielder and *Tamkp1*. (c) Spike length statistics of *Tamkp1* plants and Fielder. (d) plant length statistics of *Tamkp1* plants and Fielder. (e) 1000 grain weight statistics of *Tamkp1* plants and Fielder.

Discussion

Crop diseases are one of the major factors that significantly affect the yield and quality of wheat. The exact role of *TaMKP1* in the interaction between wheat and fungus remains unknown. In this study, we cloned and functionally characterized *MKP1* from wheat. We also proved that TaMKP1 interacts with TaMPK3/4/6. Importantly, we successfully generated *Tamkp1* plants by CRISPR-Cas9 technology and confirmed their resistance to *Pst* and *Bgt*. Our results demonstrated that simultaneous knock-out of all three homologues of *TaMKP1* confers resistance to stripe rust, *TaMKP1d* plays a greater role than other homologues.

In rice, OsMAPKKε promotes the OsMKK4–OsMAPK3/6 cascade, and thus, the ability to perceive chitin and resistance to rice blast fungus was improved (Wang *et al.*, 2017). OsILA1, indentified as a negative regulator of the OsMAPKK4–OsMAPK6 cascade and is involved in rice–*Xoo* interactions (Chen *et al.*, 2021). OsMAPK6-OsLIC-OsWRKY30 module is an immune signalling pathway in response to the bacterial pathogens (Wang *et al.*, 2022a). Interestingly, SCRE6 interacts with and dephosphorylates the OsMPK6 in rice, thereby suppressing plant immunity (Zheng *et al.*, 2022). This study suggested that pathogens can exploit the tyrosine phosphatase family to inhibit the MAPK pathway, facilitating their infection. The MAPK

pathway is also associated with plant yield. OsMKKK10, OsMKK4, and OsMAPK6 function in a common pathway to regulate grain size (Xu *et al.*, 2018a). *OsMAPK6* plays a key role in rice grain size through cell proliferation, brassinosteroids (BR) signalling, and homeostasis (Liu *et al.*, 2015). Loss of function mutations in *OsMKP1* results in larger grains, *OsMKP1* determines grain size by restricting cell proliferation in grain hulls. *OsMKP1* is a key factor influencing grain size by affecting *OsMAPK6* (Xu *et al.*, 2018b). In *Arabidopsis*, *AtMKP1* negatively regulates *MPK6*-mediated PAMP responses and resistance against bacteria, *AtMPK6*, but not *AtMPK3*, is necessary for the *mkp1*-dependent increase in resistance to *Pseudomonas syringae* pv. *tomato* DC3000 (Anderson *et al.*, 2011), and AtMKP1 was phosphorylated by AtMPK6 (Park *et al.*, 2011). Activation of the MPK3 and MPK6 is sufficient to trigger pipecolic acid production and mount systemic acquired resistance (SAR) (Wang *et al.*, 2018b). Pathogen-responsive MPK3/MPK6 cascade is an essential signalling pathway that control, respectively, the organic acid metabolism, a main branch of osmotic regulation in guard cells that function interdependently to control stomatal opening/closure, whichis is essential for stomatal immunity (Su *et al.*, 2017). A study pointed out that MPK3/MPK6 cascade is a key hub in orchestrating the trade-off between growth and defence (Su *et al.*, 2018). *NtMKP1* negatively regulates wound response and resistance against both

necrotrophic pathogens and herbivorous insects by suppression of jasmonic acid (JA) or ethylene (ET) pathways via inactivation of MAPK (Oka *et al*., 2013). In contrast, silencing of *NbMKP1* increased the accumulation of *Bamboo mosaic virus* and *Foxtail mosaic virus* (Lee *et al*., 2018). Other studies have found that substrates for MPK3/6 play important roles downstream of the MPK3/MPK6 cascade in regulating plant immunity and yield. However, these mechanisms have yet to be fully understood in wheat. In general, these studies demonstrated that MAPK kinases play important roles between plant immunity and yield. Understanding the regulatory mechanism of MAPKs will undoubtedly benefit the development of future crop varieties by providing durable resistance against pathogens and other agronomic traits (Zhang *et al*., 2023).

In our study, *TaMKP1* was found to negatively regulate the disease resistance of wheat, and TaMKP1 directly interacts with and dephosphorylates TaMPK3/4/6 (Figures 6 and S8). Interestingly, *Tamkp1* plants showed corresponding improvements in plant height and yield, the relative expression of *TaMPK6* was upregulated in *TaMKP1* knockout plants (Figure 6f), suggesting that *TaMKP1* regulates production by affecting *TaMPK6* expression. In the previous view, plants should effectively balance their immune response with growth and development. Excessive and intense immune activity can have deleterious effects on plant production, leading to defects and reduced yields. (Lozano-Duran and Zipfel, 2015; Ning *et al*., 2017). However, some studies have also shown that while improving plant resistance, it does not change growth traits and even increases yield. IPA1 promotes both yield and disease resistance by sustaining a balance between growth and immunity (Wang *et al*., 2018a). Disruption of ROD1 results in resistance to a variety of pathogens, whereas the natural ROD1 allele with agroecology-specific distribution prevalent in indica rice enhances resistance without affecting yield (Gao *et al*., 2021). The knockout of *TaPsIPK1* enhances resistance to stripe rust in wheat but does not result in any significant developmental defects (Wang *et al*., 2022b). Overexpression of *TaPIP2;10* plants improved wheat resistance and grain yield (Lu *et al*., 2022). Our study demonstrated that *Tampk1* effectively enhanced disease resistance and led to a significant increase in wheat yield.

Hexaploid wheat (*T. aestivum*, genome AABBDD) is derived from a cross between tetraploid *T. turgidum* (genome AABB) and *A. tauschii* (genome DD) (Marcussen *et al*., 2014). Through genome mapping, it was found that the wheat D genome exhibits unique characteristics in terms of disease resistance, stress resistance, adaptability and quality, disease resistance and quality-related genes were significantly expanded (Luo *et al*., 2017). The close affinities of *TaMKP1* in various wheat varieties worldwide suggested that there is strong potential for the application of *TaMKP1* in promoting increased resistance and yield in wheat.

Experimental procedures

Plant materials and pathogens

Wheat cultivar Fielder, *Pst* races (CYR31, CYR32, CYR33, CYR34), and *Bgt* were used in this study. All plant materials were grown in a greenhouse under a 16-h/8-h light cycle at a constant 12 ± 2 °C. The fresh *Pst* urediniospores were rubbed using a smear method onto the first leaves. Inoculated seedlings were placed in a humidifier at 100% humidity closed and treated in the dark for 24 h and then recovered. *Bgt* maintained on wheat in a growth chamber with a 16-h/8-h light cycle, at a constant 22 ± 2 °C.

RNA extraction and gene expression analysis

Total RNA was extracted from the wheat leaves infected by *Pst*., high-quality first-strand cDNA was generated to clone *TaMKP1* homoeologs. For gene expression analysis, quantitative reverse transcription PCR (qRT-PCR) was performed on a Analytik qTOWER³G. Specific primers for each gene were designed using SnapGene, and synthesized by Sangon Biotech (https://www.sangon.com/) (Table S2). SYBR Premix Ex Taq (TaKaRa, http://www.takara-bio.com/) was used for qRT-PCR assays. The expression levels of target genes were normalized to *TaEF-1a*. The statistical significance was evaluated by Student's *t*-test ($P < 0.05$).

Virus-Induced gene silencing

The Barley stripe mosaic virus (BSMV)-based virus-induced gene silencing (VIGS) assay was performed, as described previously (Liu *et al*., 2023). Briefly, the specific fragment of *TaMKP1* were selected and connected it with BSMV:γ to form a recombinant vector. Then, BSMV:α, BSMV:β, BSMV:γ and the recombinant vector were linearized. *In vitro* transcription was performed with the linearized plasmid as the template. The BSMV mixture was applied to fully expanded Suwon11 wheat plants by rubbing. Twelve days after inoculation with BSMV, CYR34 was inoculated in the heart leaves of wheat. The feasibility was tested using the *TaPDS* as a positive control.

Yeast two-hybrid (Y2H)

The coding fragments of TaMKP1, TaMPK3, TaMPK4 and TaMPK6 were amplified through using the primers listed in Table SX and inserted into the vectors pGADT7(AD) and pGBKT7(BD) to generate AD-TaMKP1, BD-TaMPK3, BD-TaMPK4 and BD-TaMPK6. The constructed vectors were then transformed into the yeast strains Y2H gold cultured in SD-His-Leu medium. Then, the monoclonal colonies were selected and diluted with sterile ddH₂O. Then, 5 μL of each colony were coated in SD-His-Leu-Trp-Ade + X-α-gal medium for identification. pGBKT7-53 and pGADT7-T were used as positive control, and pGBKT7-Lam and pGADT7-T were used as negative control. The interaction protein pairs were confirmed according to the growth of the colony.

Bimolecular fluorescence complementation (BiFC)

The ORF of *TaMKP1*, *TaMPK3*, *TaMPK4* and *TaMPK6* were inserted into the vectors pCV-nYFP and pCV-cYFP. The recombinant vectors were transformed into *Agrobacterium tumefaciens* strain GV3101, and then co-infiltrated into *Nicotiana benthamiana* leaves in different combinations. The positive control plants were agro-infiltrated with *A. tumefaciens* carrying pCV-nYFP-AV2 and pCV-cYFP-AC1 vectors. The negative control plants were agro-infiltrated with *A. tumefaciens* carrying empty pCV-nYFP and pCV-cYFP vectors. At 2 days after infiltration, injected areas from the leaves were observed by fluorescence microscopy using a Zeiss LSM780 microscope.

Split-luciferase complementation assay

The method of LUC assay was described as previous studies (Yang *et al*., 2022a). GV3101 containing 35S:LUCᴺ-TaMKP1 constructs mixed with 35S:LUCᶜ-TaMPK3, 35S:LUCᶜ-TaMPK4 or 35S:LUCᶜ-TaMPK6 constructs at 1:1 ratio was infiltrated into *N. benthamiana* t leaves and incubated in the growth room for 48 h. 1 mM luciferin was sprayed onto the leaves for CCD imaging.

Co-immunoprecipitation (Co-IP) assays

The coding fragments of *TaMKP1*, *TaMPK3*, *TaMPK4* and *TaMPK6* were amplified through using the primers listed and inserted into the vectors pCNF3 to generate pCNF3-TaMKP1-HA, pCNF3-TaMKP3-Flag, pCNF3-TaMKP4-Flag and pCNF3-TaMKP6-Flag. Leaves infiltrated with the Agrobacterium GV3101 harbouring pCNF3-TaMKP1-HA, pCNF3-TaMKP3-Flag, pCNF3-TaMKP4-Flag and pCNF3-TaMKP6-Flag were harvested and ground into powder under liquid nitrogen at 48 hpi. Co-IP assays were conducted as described before (Wang *et al.*, 2016).

Immunoblotting

In the experiments, protein extracts from wheat leaves were fractionated through electrophoresis using a regular 12.5% w/v SDS-PAGE gel. The resulting protein blots were then subjected to hybridization with commercially obtained α-pMPK antibodies in order to ascertain the phosphorylation status of MPK3, MPK4 and MPK6 (Lu *et al.*, 2022).

Construction of the CRISPR/Cas9-related vectors

To investigate off-target effects, three sgRNA targets for *TaMKP1* were designed on the conserved domains of all three genomes of wheat based on the prediction of the WheatCrispr (https://crispr.bioinfo.nrc.ca/WheatCrispr/).

The delivered of the constructed vector into wheat immature embryos were performed as previously described (Li *et al.*, 2021). The vector contains the bar gene, the wheat leaves were ground into juice, and 200 μL ddH$_2$O was added, the bar gene test strips were used to detect whether there were positive plants.

Molecular characterization of different mutant lines

Wheat genomic DNA from leaf tissue was extracted using cetyl trimethyl ammonium bromide (CTAB) and PCR amplification was performed using PrimeSTAR® Max DNA Polymerase (https://www.takarabiomed.com.cn/) and 50–100 ng of genomic DNA as a template. To screen for mutations in the *TaMKP1* gene, suitable primers were designed for PCR amplification and sequencing based on the indicated target loci and previous research methods (Liu *et al.*, 2019). Any plant carrying not causing coding frame shift were excluded from further experiments.

3,3-diaminabenzadine (DAB) and trypan blue staining

The staining method is based on the previous method with some modifications (Melichar *et al.*, 2008). The plant tissues were stained with 0.1% DAB for 8 h. The leaves were then placed in 95% ethanol in a boiling water bath for 5 min. The leaves were placed in a saturated chloral hydrate solution for decolorisation and then photographed under the microscope when the chlorophyll had completely faded.

Plant tissues were soaked in 0.4% trypan blue staining solution and vacuum-treated for 5 min, followed by a boiling water bath for 5 min. The leaves were decolored in saturated chloral hydrate solution and photographed when the chlorophyll had completely faded.

Statistical analysis

All experiments were performed using three replicates of the biological samples. The data is presented as means ± standard deviation, and data were analysed using SPSS. Differences between those in knockdown/overexpression plants and control plants were assessed using Student's *t*-tests. Statistical significance was indicated as follows: * for $P < 0.05$, ** for $P < 0.01$, *** for $P < 0.001$, and **** for $P < 0.0001$. Inter-group variations in the bar graph depicting letter identification were examined using analysis of ANOVA and LSD Duncan. If the *P*-value was greater than 0.05, the letters were considered the same, indicating no significant difference. If the *P*-value was less than or equal to 0.05, the letters were considered different, indicating a significant difference.

Conflict of interest

The authors have no conflict of interest to declare.

Data availability statement

The data that support the findings of this study are available on request from the corresponding author. The data are not publicly available due to privacy or ethical restrictions.

References

Anderson, J.C., Bartels, S., Besteiro, M.A.G., Shahollari, B., Ulm, R. and Peck, S.C. (2011) Arabidopsis MAP Kinase Phosphatase 1 (AtMKP1) negatively regulates MPK6-mediated PAMP responses and resistance against bacteria. *Plant J.* **67**, 258–268.

Anderson, J.C., Wan, Y., Kim, Y.M., Pasa-Tolic, L., Metz, T.O. and Peck, S.C. (2014) Decreased abundance of type III secretion system-inducing signals in Arabidopsis mkp1 enhances resistance against *Pseudomonas syringae*. *Proc. Natl. Acad. Sci. U.S.A.* **111**, 6846–6851.

Bartels, S., Anderson, J.C., Gonzalez Besteiro, M.A., Carreri, A., Hirt, H., Buchala, A., Metraux, J.P. *et al.* (2009) MAP kinase phosphatase1 and protein tyrosine phosphatase1 are repressors of salicylic acid synthesis and SNC1-mediated responses in *Arabidopsis*. *Plant Cell*, **21**, 2884–2897.

Chen, J., Wang, L.H., Yang, Z.Y., Liu, H.B., Chu, C.L., Zhang, Z.Z., Zhang, Q.L. *et al.* (2021) The rice Raf-like MAPKKK OsILA1 confers broad-spectrum resistance to bacterial blight by suppressing the OsMAPKK4-OsMAPK6 cascade. *J. Integr. Plant Biol.* **63**, 1815–1832.

Chen, Y.M., Guo, Y.W., Guan, P.F., Wang, Y.F., Wang, X.B., Wang, Z.H., Qin, Z. *et al.* (2023) A wheat integrative regulatory network from large-scale complementary functional datasets enables trait-associated gene discovery for crop improvement. *Mol. Plant* **16**, 393–414.

Devendrakumar, K.T., Li, X. and Zhang, Y.L. (2018) MAP kinase signalling: interplays between plant PAMP- and effector-triggered immunity. *Cell. Mol. Life Sci.* **75**, 2981–2989.

Dodds, P.N. and Rathjen, J.P. (2010) Plant immunity: towards an integrated view of plant-pathogen interactions. *Nat. Rev. Genet.* **11**, 539–548.

Escudero, V., Torres, M.A., Delgado, M., Sopena-Torres, S., Swami, S., Morales, J., Munoz-Barrios, A. *et al.* (2019) Mitogen-activated protein kinase phosphatase 1 (MKP1) negatively regulates the production of reactive oxygen species during *Arabidopsis* immune responses. *Mol. Plant Microbe. In.* **32**, 464–478.

Gao, M., He, Y., Yin, X., Zhong, X., Yan, B., Wu, Y., Chen, J. *et al.* (2021) Ca^{2+} sensor-mediated ROS scavenging suppresses rice immunity and is exploited by a fungal effector. *Cell*, **184**, 5391–5404.e5317.

Ghorbel, M., Cotelle, V., Ebel, C., Zaidi, I., Ormancey, M., Galaud, J.P. and Hanin, M. (2017) Regulation of the wheat MAP kinase phosphatase 1 by 14-3-3 proteins. *Plant Sci.* **257**, 37–47.

Ghorbel, M., Zaidi, I., Ebel, C. and Hanin, M. (2019) Differential regulation of the durum wheat MAPK phosphatase 1 by calmodulin, bivalent cations and possibly mitogen activated protein kinase 3. *Plant Physiol. Biochem.* **135**, 242–252.

Huot, B., Yao, J., Montgomery, B.L. and He, S.Y. (2014) Growth–defense tradeoffs in plants: a balancing act to optimize fitness. *Mol. Plant*, **7**, 1267–1287.

Ichimura, K., Shinozaki, K., Tena, G., Sheen, J., Henry, Y., Champion, A., Kreis, M. *et al.* (2002) Mitogen-activated protein kinase cascades in plants: a new nomenclature. *Trends Plant Sci.* **7**, 301–308.

Jiang, L.Y., Anderson, J.C., Besteiro, M.A.G. and Peck, S.C. (2017) Phosphorylation of *Arabidopsis* MAP kinase phosphatase 1 (MKP1) is required for PAMP responses and resistance against bacteria. *Plant Physiol.* **175**, 1839–1852.

Keyse, S.M. (2000) Protein phosphatases and the regulation of mitogen-activated protein kinase signalling. *Curr. Opin. Cell Biol.* **12**, 186–192.

Kim, H.S. and Asmis, R. (2017) Mitogen-activated protein kinase phosphatase 1 (MKP-1) in macrophage biology and cardiovascular disease. A redox-regulated master controller of monocyte function and macrophage phenotype. *Free Radic. Biol. Med.* **109**, 75–83.

Lee, C.C., Wu, Y.J., Hsueh, C.H., Huang, Y.T., Hsu, Y.H. and Meng, M.H. (2018) Mitogen-activated protein kinase phosphatase 1 reduces the replication efficiency of *Bamboo mosaic virus* in *Nicotiana benthamiana*. *Mol. Plant Pathol.* **19**, 2319–2332.

Li, P., Lu, Y.J., Chen, H. and Day, B. (2020) The lifecycle of the plant immune system. *Crit. Rev. Plant Sci.* **39**, 72–100.

Li, J.H., Zhang, S.J., Zhang, R.Z., Gao, J., Qi, Y.P., Song, G.Q., Li, W. *et al.* (2021) Efficient multiplex genome editing by CRISPR/Cas9 in common wheat. *Plant Biotechnol. J.* **19**, 427–429.

Lin, H., Wang, M., Chen, Y., Nomura, K., Hui, S., Gui, J., Zhang, X. *et al.* (2022) An MKP-MAPK protein phosphorylation cascade controls vascular immunity in plants. *Sci. Adv.* **8**, eabg8723.

Liu, S.Y., Hua, L., Dong, S.J., Chen, H.Q., Zhu, X.D., Jiang, J.E., Zhang, F. *et al.* (2015) OsMAPK6, a mitogen-activated protein kinase, influences rice grain size and biomass production. *Plant J.* **84**, 672–681.

Liu, Q., Wang, C., Jiao, X.Z., Zhang, H.W., Song, L.L., Li, Y.X., Gao, C.X. *et al.* (2019) Hi-TOM: a platform for high-throughput tracking of mutations induced by CRISPR/Cas systems. *Sci. China Life Sci.* **62**, 1–7.

Liu, S., Xiao, M., Fang, A., Tian, B., Yu, Y., Bi, C., Ma, D. *et al.* (2023) LysM proteins TaCEBiP and TaLYK5 are involved in immune responses mediated by chitin coreceptor TaCERK1 in wheat. *J. Agric. Food Chem.* **71**, 13535–13545.

Long, Y.P., Xie, D.J., Zhao, Y.Y., Shi, D.Q. and Yang, W.C. (2019) BICELLULAR POLLEN 1 is a modulator of DNA replication and pollen development in *Arabidopsis*. *New Phytol.* **222**, 588–603.

Lozano-Duran, R. and Zipfel, C. (2015) Trade-off between growth and immunity: role of brassinosteroids. *Trends Plant Sci.* **20**, 12–19.

Lu, K., Chen, X.C., Yao, X.H., An, Y.Y., Wang, X., Qin, L.N., Li, X.X. *et al.* (2022) Phosphorylation of a wheat aquaporin at two sites enhances both plant growth and defense. *Mol. Plant*, **15**, 1772–1789.

Luo, M.-C., Gu, Y.Q., Puiu, D., Wang, H., Twardziok, S.O., Deal, K.R., Huo, N. *et al.* (2017) Genome sequence of the progenitor of the wheat D genome *Aegilops tauschii*. *Nature*, **551**, 498–502.

Marcussen, T., Sandve, S.R., Heier, L., Spannagl, M., Pfeifer, M., International Wheat Genome Sequencing Consortium, Jakobsen, K.S. *et al.* (2014) Ancient hybridizations among the ancestral genomes of bread wheat. *Science*, **345**, 1250092.

Melichar, J.P.E., Berry, S., Newell, C., MacCormack, R. and Boyd, L.A. (2008) QTL identification and microphenotype characterisation of the developmentally regulated yellow rust resistance in the UK wheat cultivar Guardian. *Theor. Appl. Genet.* **117**, 391–399.

Monaghan, J. and Zipfel, C. (2012) Plant pattern recognition receptor complexes at the plasma membrane. *Curr. Opin. Plant Biol.* **15**, 349–357.

Ning, Y.S., Liu, W.D. and Wang, G.L. (2017) Balancing immunity and yield in crop plants. *Trends Plant Sci.* **22**, 1069–1079.

Oka, K., Amano, Y., Katou, S., Seo, S., Kawazu, K., Mochizuki, A., Kuchitsu, K. *et al.* (2013) Tobacco MAP kinase phosphatase (NtMKP1) negatively regulates wound response and induced resistance against Necrotrophic Pathogens and Lepidopteran Herbivores. *Mol Plant Microbe In* **26**, 668–675.

Park, H.C., Song, E.H., Nguyen, X.C., Lee, K., Kim, K.E., Kim, H.S., Lee, S.M. *et al.* (2011) *Arabidopsis* MAP kinase phosphatase 1 is phosphorylated and activated by its substrate AtMPK6. *Plant Cell Rep.* **30**, 1523–1531.

Schwessinger, B. and Ronald, P.C. (2012) Plant innate immunity: perception of conserved microbial signatures. *Annu. Rev. Plant Biol.* **63**, 451–482.

Su, J.B., Zhang, M.M., Zhang, L., Sun, T.F., Liu, Y.D., Lukowitz, W., Xu, J. *et al.* (2017) Regulation of stomatal immunity by interdependent functions of a pathogen-responsive MPK3/MPK6 cascade and abscisic Acid. *Plant Cell* **29**, 526–542.

Su, J., Yang, L., Zhu, Q., Wu, H., He, Y., Liu, Y., Xu, J. *et al.* (2018) Active photosynthetic inhibition mediated by MPK3/MPK6 is critical to effector-triggered immunity. *PLoS Biol.* **16**, e2004122.

Sun, T., Nitta, Y., Zhang, Q., Wu, D., Tian, H., Lee, J.S. and Zhang, Y. (2018) Antagonistic interactions between two MAP kinase cascades in plant development and immune signaling. *EMBO Rep.* **19**, e45324.

Takahashi, F., Mizoguchi, T., Yoshida, R., Ichimura, K. and Shinozaki, K. (2011) Calmodulin-dependent activation of MAP kinase for ROS homeostasis in *Arabidopsis*. *Mol. Cell*, **41**, 649–660.

Teixeira, P.J.P., Colaianni, N.R., Fitzpatrick, C.R. and Dangl, J.L. (2019) Beyond pathogens: microbiota interactions with the plant immune system. *Curr. Opin. Microbiol.* **49**, 7–17.

Uchida, K., Yamaguchi, M., Kanamori, K., Ariga, H., Isono, K., Kajino, T., Tanaka, K. *et al.* (2022) MAP KINASE PHOSPHATASE1 promotes osmotolerance by suppressing PHYTOALEXIN DEFICIENT4-independent immunity. *Plant Physiol.* **189**, 1128–1138.

Ulm, R., Revenkova, E., di Sansebastiano, G.P., Bechtold, N. and Paszkowski, J. (2001) Mitogen-activated protein kinase phosphatase is required for genotoxic stress relief in. *Genes Dev.* **15**, 699–709.

Ulm, R., Ichimura, K., Mizoguchi, T., Peck, S.C., Zhu, T., Wang, X., Shinozaki, K. *et al.* (2002) Distinct regulation of salinity and genotoxic stress responses by *Arabidopsis* MAP kinase phosphatase 1. *EMBO J.* **21**, 6483–6493.

Wang, Z., Li, N., Jiang, S., Gonzalez, N., Huang, X., Wang, Y., Inzé, D. *et al.* (2016) SCFSAP controls organ size by targeting PPD proteins for degradation in *Arabidopsis thaliana*. *Nat. Commun.* **7**, 11192.

Wang, C., Wang, G., Zhang, C., Zhu, P.K., Dai, H.L., Yu, N., He, Z.H. *et al.* (2017) OsCERK1-mediated chitin perception and immune signaling requires receptor-like cytoplasmic kinase 185 to activate an MAPK cascade in rice. *Mol. Plant* **10**, 619–633.

Wang, J., Zhou, L., Shi, H., Chern, M., Yu, H., Yi, H., He, M. *et al.* (2018a) A single transcription factor promotes both yield and immunity in rice. *Science*, **361**, 1026–1028.

Wang, Y.M., Schuck, S., Wu, J.N., Yang, P., Doring, A.C., Zeier, J. and Tsuda, K. (2018b) A MPK3/6-WRKY33-ALD1-pipecolic acid regulatory loop contributes to systemic acquired resistance. *Plant Cell*, **30**, 2480–2494.

Wang, R.Y., He, F., Ning, Y.S. and Wang, G.L. (2020) Fine-Tuning of RBOH-Mediated ROS Signaling in Plant Immunity. *Trends Plant Sci.* **25**, 1060–1062.

Wang, L.H., Chen, J., Zhao, Y.Q., Wang, S.P. and Yuan, M. (2022a) OsMAPK6 phosphorylates a zinc finger protein OsLIC to promote downstream OsWRKY30 for rice resistance to bacterial blight and leaf streak. *J. Integr. Plant Biol.* **64**, 1116–1130.

Wang, N., Tang, C., Fan, X., He, M., Gan, P., Zhang, S., Hu, Z. *et al.* (2022b) Inactivation of a wheat protein kinase gene confers broad-spectrum resistance to rust fungi. *Cell* **185**, 2961–2974.e2919.

Wang, Z., Li, X., Yao, X., Ma, J., Lu, K., An, Y., Sun, Z. *et al.* (2023) MYB44 regulates PTI by promoting the expression of EIN2 and MPK3/6 in Arabidopsis. *Plant Commun.* **4**, 100628.

Xu, R., Duan, P.G., Yu, H.Y., Zhou, Z.K., Zhang, B.L., Wang, R.C., Li, J. *et al.* (2018a) Control of grain size and weight by the OsMKKK10-OsMKK4-OsMAPK6 signaling pathway in Rice. *Mol. Plant* **11**, 860–873.

Xu, R., Yu, H.Y., Wang, J.M., Duan, P.G., Zhang, B.L., Li, J., Li, Y. *et al.* (2018b) A mitogen-activated protein kinase phosphatase influences grain size and weight in rice. *Plant J.* **95**, 937–946.

Yang, S., Cai, W.W., Shen, L., Cao, J.S., Liu, C.L., Hu, J., Guan, D.Y. *et al.* (2022a) A CaCDPK29-CaWRKY27b module promotes CaWRKY40-mediated thermotolerance and immunity to *Ralstonia solanacearum* in pepper. *New Phytol.* **233**, 1843–1863.

Yang, Z.Z., Wang, Z.H., Wang, W.X., Xie, X.M., Chai, L.L., Wang, X.B., Feng, X.B. *et al.* (2022b) ggComp enables dissection of germplasm resources and construction of a multiscale germplasm network in wheat. *Plant Physiol.* **188**, 1950–1965.

Zaidi, I., Ebel, C., Belgaroui, N., Ghorbel, M., Amara, I. and Hanin, M. (2016) The wheat MAP kinase phosphatase 1 alleviates salt stress and increases antioxidant activities in Arabidopsis. *J. Plant Physiol.* **193**, 12–21.

Zhang, S.Q. and Klessig, D.F. (2001) MAPK cascades in plant defense signaling. *Trends Plant Sci.* **6**, 520–527.

Zhang, M.M., Su, J.B., Zhang, Y., Xu, J. and Zhang, S.Q. (2018) Conveying endogenous and exogenous signals: MAPK cascades in plant growth and defense. *Curr. Opin. Plant Biol.* **45**, 1–10.

Zhang, T.Y., Li, Z.Q., Zhao, Y.D., Shen, W.J., Chen, M.S., Gao, H.Q., Ge, X.M. *et al.* (2021) Ethylene-induced stomatal closure is mediated via MKK1/3-MPK3/6 cascade to EIN2 and EIN3. *J. Integr. Plant Biol.* **63**, 1324–1340.

Zhang, D.D., Lv, B. and Qiu, J.L. (2022) Being tough: The secret weapon of plants against vascular pathogens. *Mol. Plant*, **15**, 934–936.

Zhang, H., Liu, Y., Zhang, X., Ji, W. and Kang, Z. (2023) A necessary considering factor for breeding: growth-defense tradeoff in plants. *Stress Biol.* **3**, 6.

Zheng, X.H., Fang, A.F., Qiu, S.S., Zhao, G.S., Wang, J.Y., Wang, S.Z., Wei, J.J. *et al.* (2022) *Ustilaginoidea virens* secretes a family of phosphatases that stabilize the negative immune regulator OsMPK6 and suppress plant immunity. *Plant Cell*, **34**, 3088–3109.

Zhou, J.M. and Zhang, Y.L. (2020) Plant immunity: danger perception and signaling. *Cell*, **181**, 978–989.

Supporting information

Additional supporting information may be found online in the Supporting Information section at the end of the article.

Table S1 TaMKP1 gene regulatory relationship.
Table S2 Primers used in this study.
Figure S1 Alignment and analysis of nucleotide sequences of three homologous of *TaMKP1* and *AtMKP1*.
Figure S2 Expression levels of *TaMKP1* in different tissues.
Figure S3 The *Bar* gene test strip is used to screen for positive mutants.
Figure S4 Sequence information for the *Tamkp1* mutant.
Figure S5 Effects of chitin and flg22 on stimulating ROS production in *Tamkp1* plants.
Figure S6 Analysis of wheat MAPKs-like MAPK cascade pathway genes.
Figure S7 *TaMKP1* gene regulatory network and global germplasm relationships.
Figure S8 TaMKP1 negatively regulates wheat disease resistance by inhibiting TaMPK3/4/6.